




Lower blastocyst quality after conventional vs. Piezo ICSI in the horse reflects delayed sperm component remodeling and oocyte activation

R. M. Salgado¹ · J. G. Brom-de-Luna¹ · H. L. Resende¹ · H. S. Canesin¹ · Katrin Hinrichs¹ 

Received: 1 December 2017 / Accepted: 27 March 2018 / Published online: 10 April 2018
© Springer Science+Business Media, LLC, part of Springer Nature 2018

Abstract

Purpose The aim of this study was to evaluate the differential effects of conventional and Piezo-driven ICSI on blastocyst development, and on sperm component remodeling and oocyte activation, in an equine model.

Methods In vitro-matured equine oocytes underwent conventional (Conv) or Piezo ICSI, the latter utilizing fluorocarbon ballast. Blastocyst development was compared between treatments to validate the model. Then, oocytes were fixed at 0, 6, or 18 h after injection, and stained for the sperm tail, acrosome, oocyte cortical granules, and chromatin. These parameters were compared between injection techniques and between sham-injected and sperm-injected oocytes among time periods.

Results Blastocyst rates were 39 and 40%. The nucleus number was lower, and the nuclear fragmentation rate was higher, in blastocysts produced by Conv. Cortical granule loss started at 0h after both sperm and sham injection. The acrosome was present at 0h in both ICSI treatments, and persisted to 18h in significantly more Conv than Piezo oocytes (72 vs. 21%). Sperm head area was unchanged at 6h in Conv but significantly increased at this time in Piezo; correspondingly, at 6h significantly more Conv than Piezo oocytes remained at MII (80 vs. 9.5%). Sham injection did not induce significant meiotic resumption.

Conclusions These data show that Piezo ICSI is associated with more rapid sperm component remodeling and oocyte meiotic resumption after sperm injection than is conventional ICSI, and with higher embryo quality at the blastocyst stage. This suggests that there is value in exploring the Piezo technique, utilized with a non-toxic fluorocarbon ballast, for use in clinical human ICSI.

Keywords Intracytoplasmic sperm injection · Fertilization · Oocyte · Sperm · Horse · Blastocyst · Acrosome · Cortical granules · Embryo

Introduction

Intracytoplasmic sperm injection (ICSI) has become an important method for producing embryos in vitro in several species, including humans, because it provides high fertilization rates and allows utilization of semen samples with few sperm or

sperm of low quality [1–4]. ICSI is the most effective method applicable to fertilization with immotile sperm or immature spermatids (review; [5]). There are two main methods for performing ICSI: conventional and Piezo-driven (Piezo). In conventional ICSI, a sharp micropipette is used to crush the sperm tail to rupture the sperm plasma membrane and thus immobilize the sperm, then to penetrate the zona pellucida and the oolemma. In Piezo ICSI, a blunt injection micropipette uses Piezo-driven microvibrations to rupture the sperm plasma membrane and to penetrate the zona and oolemma [6].

Using the mouse model, Piezo-assisted ICSI was first reported by Kimura and Yanagimachi [6] who found that this technique significantly increased rates of oocyte survival after sperm injection (80 vs. 16% for conventional ICSI), and also increased blastocyst rates in surviving oocytes. These authors hypothesized that improvement in success with Piezo in the mouse was due to decreased damage to the oolemma and cytoplasm. The action of the Piezo-electric vibrations on the sperm plasma membrane and acrosome may also affect

This work was supported by the Clinical Equine ICSI Program, Texas A&M University, and the Link Equine Research Fund, Texas A&M University.

A portion of these data were presented at the 2018 annual meeting of the International Embryo Technology Society, and appears as a 500-word abstract in the Proceedings of that meeting.

✉ Katrin Hinrichs
khinrichs@cvm.tamu.edu

¹ Department of Veterinary Physiology & Pharmacology, College of Veterinary Medicine & Biomedical Sciences, Texas A&M University, TAMU 4466, College Station, TX 77843-4466, USA

results. Sperm immobilized by Piezo have been shown to stain more rapidly with membrane-impermeable stains than do sperm immobilized by the conventional technique (5 vs. 42 s in human sperm [7]; 26 vs. 76 s in pig sperm [8]), suggesting that membrane dissolution is more rapid with Piezo. It could be assumed that membrane dissolution is necessary for the efflux of oocyte-activating factors from the sperm after injection. In a study in sheep, Anzalone and coworkers [9] found that 46% of sperm had acrosomal disruption after Piezo manipulation, and concluded that acrosomal loss before ICSI was required for embryonic development. Removal of the acrosome with calcium ionophore, methyl- β cyclodextrin, or lysolethicin before ICSI has been shown to enhance embryo development or viability in several species (mouse [10, 11]; rat [12]; cattle [13]; sheep [9]). Thus, if the high incidence of acrosome removal by the Piezo technique was repeatable, this would be a major advantage to using the Piezo for ICSI.

In the human, conventional ICSI is associated with high rates of oocyte survival and embryo development, thus investigation of alternative micromanipulation methods has been limited. Implementing the Piezo technique would involve need for additional equipment and expertise. Furthermore, the Piezo-driven pipette typically contains mercury, a potential neurotoxin, which is problematic for clinical use. However, it is possible that use of the Piezo may convey advantages for human ICSI. Retrospective studies from clinical human programs using conventional and Piezo ICSI (the latter utilizing mercury) indicated that use of the Piezo drill resulted in higher pronucleus (PN) formation and higher pregnancy or live birth rates [14, 15]. In a similar retrospective study, using Piezo injection with a nontoxic fluorocarbon-based fluid instead of mercury, and an ultrathin-walled pipette, significantly higher PN formation and pregnancy rates were found for Piezo vs. conventional ICSI [16].

Investigation of the mechanisms underlying a possible difference in embryo development after ICSI with the two techniques has been challenging. On the one hand, obtaining normal human oocytes for research purposes has numerous limitations; on the other, unfortunately, in many domestic and laboratory animal species, a direct comparison of conventional and Piezo ICSI is difficult because ICSI is not associated with high rates of embryonic development or requires use of the Piezo drill, sperm pre-treatment, or exogenous activation [6, 8, 17–19]. For example, in the pig, Katayama et al. [8] found that use of the Piezo drill was associated with increased disruption of the sperm plasma membrane, and promoted greater dissolution of the sperm perinuclear theca and formation of normal male PN after ICSI, compared with the conventional technique. In that study, the rate of PN formation was significantly higher for Piezo than for conventional ICSI; however, only 48 and 29% of injected oocytes, respectively, formed two PN, and further embryo development was not evaluated. In this light, the horse may provide an excellent model for such investigation. ICSI has been used in clinical

assisted reproductive technology (ART) programs in the horse for over a decade [3, 20–22], and has been conducted using both Piezo [23–26] and conventional [27–31] techniques, although they have not been critically compared. Furthermore, the mare has been suggested as a relevant model for the study of oocyte and follicle biology; mares are monovulatory and their follicular development, oocyte maturation kinetics, and response to reproductive aging closely resemble those of women [32, 33]. To the best of our knowledge, morphokinetic parameters of post-fertilization development, including acrosome status, chromatin decondensation, meiotic resumption, and cortical granule exocytosis, have not been directly compared over time after ICSI in a system validated to respond to both techniques. Thus, the horse model could be used to evaluate differences between conventional and Piezo ICSI, the results of which may reflect the outcome in a human system.

The purpose of this study was to compare blastocyst development after conventional and Piezo ICSI in an equine system, then to compare the morphokinetics of sperm component remodeling and oocyte activation between oocytes fertilized using these two techniques. Based on the reported greater disruption of the sperm plasma membrane, and ease of penetration of the oolemma, associated with use of the Piezo in other species [6, 8], we hypothesized that use of the Piezo would result in a higher blastocyst rate than that for conventional ICSI, associated with greater loss of the acrosome before injection, and a higher proportion of sperm showing decondensation and normal PN formation after injection.

Materials and methods

Experimental design

Blastocyst formation after conventional and Piezo ICSI

In vitro-matured oocytes were subjected to conventional (Conv) or Piezo ICSI, and cultured for embryo development in vitro. Embryos were evaluated on days 7 to 10 after ICSI for evidence of development to blastocyst, and presumptive blastocysts were fixed and stained with DAPI on the day of identification to confirm the stage of development. Cleavage and blastocyst rates, and the proportion of blastocysts developing on different days of culture, were compared between treatments. The number of healthy nuclei and the nuclear fragmentation rate in DAPI-stained blastocysts were compared between treatments.

Comparison of kinetics of sperm processing and oocyte activation after conventional or Piezo ICSI

For this experiment, sperm mitochondria were stained with a mitochondrial stain during the swim-up procedure. In vitro-matured oocytes were subjected to Conv or Piezo ICSI, were

sham-injected (injected with medium without sperm) or were placed in the ICSI dish but not injected. The uninjected oocytes were fixed immediately after the ICSI session was completed (Uninj 0H group), or were cultured for 18 h, then fixed (Uninj 18H group). Sperm-injected (Conv and Piezo) and Sham-injected (Sham-Conv and Sham-Piezo) oocytes were fixed either immediately after the ICSI session was completed (0H groups) or were cultured for 6 or 18 h, then fixed (6H and 18H groups).

Fixed oocytes were stained with peanut agglutinin (PNA) and DAPI, then photomicrographs were obtained using an inverted fluorescence microscope and a confocal microscope. Photomicrographs of each oocyte were evaluated for sperm head area, presence and location of sperm tail and acrosome, the status of cortical granules (CG), stage of the oocyte chromatin, number and status of pronuclei (PN), and the presence of cytoplasmic extrusions in the perivitelline space.

General methods

For all experiments, Conv and Piezo injections were performed concurrently by separate experienced operators (RMS and JBdL). All experimental procedures were performed according to the *United States Government Principles for the Utilization and Care of Vertebrate Animals Used in Testing, Research and Training* and were approved by the Institutional Animal Care and Use Committee (IACUC AUP 2015-0282) at Texas A&M University.

Oocyte recovery

Immature oocytes were collected by transvaginal ultrasound-guided follicle aspiration (TVA) from a research herd of 16 Quarter-type mares, as previously described [34]. Aspiration and flushing of all follicles ≥ 5 mm diameter were performed using a commercial complete embryo flush solution (Complete Flush, Vigro, Vetoquinol, Fort Worth, TX, USA) supplemented with 8 IU/ml heparin (Sigma-Aldrich Co., St. Louis, MO, USA). The aspirated fluid and follicular contents were filtered through an embryo filter (EmCon filter, Immuno Systems, Inc., Spring Valley, WI, USA), and the cumulus-oocyte complexes (COCs) were recovered from the collected cellular material. The COCs were washed twice in commercial equine embryo holding medium (Vigro, Vetoquinol), placed in 1.1-ml borosilicate glass vials filled with this medium, and held overnight at room temperature (~ 22 °C) protected from light. Overnight holding under these conditions maintains meiotic arrest [35, 36] and allows synchronization of the onset of maturation of all oocytes recovered on a given day. Additionally, the ability to place oocytes into maturation culture early the next morning facilitates scheduling of micromanipulation procedures. Overnight room-temperature holding of equine oocytes has been shown to have no detrimental effect on equine oocyte maturation or blastocyst rates [26, 35].

Oocyte in vitro maturation

After overnight holding, vials were warmed to 38 °C. The COCs were removed and placed in 150- μ l droplets of equilibrated maturation medium consisting of M199 with Earle's salts (Invitrogen, Carlsbad, CA, USA) supplemented with 10% fetal bovine serum (FBS; Invitrogen), 5 mU FSH (Sioux Biochemicals, Sioux Center, IA, USA), and 25 μ g/ml gentamicin (Invitrogen), under light mineral oil (Sage, Trumbull, CT, USA), with a maximum of 15 oocytes per droplet. The COCs were cultured at 38.2 °C in a humidified atmosphere of 5% CO₂ in air. After 24 to 28 h in maturation culture, oocytes were denuded of cumulus. Those oocytes having a polar body were divided into two groups by a third party, and the groups were randomly allocated to Conv or Piezo ICSI or sham-injection treatments.

Sperm preparation

Frozen-thawed semen from the same fertile stallion was used for all ICSI experiments. Sperm were prepared for ICSI via swim-up. For this, 200 μ l of thawed semen was layered under 1 ml of GMOPS (Vitrolife, Englewood, CO, USA) with 10% added FBS and incubated at 38 °C for 20 min. After incubation, the top 0.6 ml of the medium was collected and centrifuged at 400 \times g for 3 min. The supernatant was removed and the pellet was resuspended in 1 ml GMOPS/FBS and centrifuged again. The supernatant was removed and the sperm pellet was mixed with the remaining ~ 20 μ l of medium.

Micromanipulation procedures

Two sets of equipment were used, one for each technique. Both sets incorporated the same make of inverted microscope (Axiovert; Zeiss, Oberkochen, Germany) and micromanipulators (TransferMan NK; Eppendorf, Hauppauge, NY, USA). For Piezo ICSI, we used a PMAS-CT150 Piezo drill (Prime Tech, Japan) and a pipette filled with non-toxic fluorocarbon ballast (Fluorinert FC-770, Sigma-Aldrich, St. Louis, MO, USA).

Microinjections were carried out at $\times 200$ magnification, with the stage warmers set at 37.5 °C. For micromanipulation, a 50 \times 9-mm (Conv) or 100 \times 20-mm (Piezo) Petri dish was used and droplets were made under oil. For the sperm droplet, medium containing 7% PVP was prepared by mixing 14 μ l of a commercial 10% PVP solution (PVP, LifeGlobal, Guilford, CT, USA) with 6 μ l of GMOPS/FBS, and a 5- μ l droplet of this medium was placed in the micromanipulation dish. One microliter of the resuspended sperm pellet was placed on the surface of this droplet, and motile sperm were identified after swimming down into the droplet. The oocytes were held in separate 5- μ l droplets (one oocyte per droplet) of M199/Hanks' salts with 10% FBS. During micromanipulation,

the oocyte was held with a holding pipette (VacuTip, Eppendorf; inner diameter 15 μm , outer diameter, 100 μm , angle 35°).

Conventional ICSI

For each injection, a motile sperm in the sperm droplet was immobilized by rolling its tail rapidly against the bottom surface of the dish with the injection pipette (TransferTip-RP, Eppendorf; internal diameter 4 μm , outer diameter 7 μm , and angle 35°). Membrane breakage was assumed when the sperm became immobile. The immobilized sperm was then aspirated tail-first into the injection pipette, and the pipette was moved to the oocyte droplet. The oocyte was held with the polar body at either 6:00 or 12:00, whichever presented the clearest cytoplasm in the aspect of the oocyte closest to the holding pipette. The sperm was advanced within the injection pipette until it was near the tip. The injection pipette was introduced through the zona pellucida and advanced into the oocyte until close to the opposite side of the oocyte, i.e., advanced through approximately 90% of the oocyte diameter. Suction was applied to break the oolemma, which was confirmed when cytoplasm was rapidly aspirated into the pipette, then the sperm was ejected into the cytoplasm with a minimum of medium.

Piezo-driven ICSI

For Piezo ICSI, the micropipette had a blunt tip and a 6- μm inner diameter (Piezo Drill Tip Mouse ICSI, Eppendorf; angle 25°), and before use was completely filled with Fluorinert FC-770, using a loading pipette. The initial settings for immobilizing the sperm and breaching the zona were speed 5, intensity 9; the initial settings for penetrating the oolemma were speed 3, intensity 7. These were adjusted when necessary based on the response of the sperm and oocyte during manipulation. The injection pipette was placed into the sperm droplet and a motile sperm was aspirated tail-first into the pipette. The sperm was then advanced slowly out of the pipette and as the midpiece exited the pipette, the pipette was moved to contact the sperm and Piezo pulses were applied. This procedure was repeated, then the immobilized sperm was drawn back entirely into the injection pipette and the pipette was moved to the oocyte droplet. The oocyte was held with the polar body at either 6:00 or 12:00, whichever presented the clearest cytoplasm in the aspect of the oocyte closest to the holding pipette. A core of zona pellucida was removed using the injection pipette under pulses from the Piezo drill. The sperm was then advanced within the injection pipette until it was near the tip. The pipette was introduced through the hole in the zona, and was advanced into the oocyte until close to the opposite side of the oocyte, i.e., advanced through approximately 90% of the oocyte

diameter. A Piezo pulse was applied to break the oolemma and, without aspiration of cytoplasm into the pipette, the sperm was ejected into the cytoplasm.

Sham injection

For sham injection, dishes were set up as for ICSI, with the exception that 1 μL of GMOPS/FBS without sperm was added to the 5 μL droplet of 7% PVP. An amount of this medium equivalent to that typically accompanying a sperm at the time of injection was picked up in the micropipette and injected into the oocyte cytoplasm as described for Conv or Piezo, above.

Culture for blastocyst formation

Injected oocytes were held in M199/Earle's salts with 10% FBS in 5% CO_2 in air at 38.2 °C for approximately 40 min after injection. After the post-injection holding period, the injected oocytes were transferred to and cultured in a commercial human embryo culture medium (Global medium, LifeGlobal, Guilford, CT, USA) supplemented with 10% FBS, in droplets under oil, at a ratio of 5 to 7.5 μL medium/oocyte, with 2–4 embryos per droplet. The culture environment was 6% CO_2 , 5% O_2 , and 89% N_2 at 38.2 °C. At day 5, cleavage was evaluated and cleaved embryos were transferred to droplets of DMEM/F-12 (Sigma-Aldrich, #D-6421) supplemented with 6 ml/L 1 N NaOH, 2.5 mM glycyl-glutamine (Sigma-Aldrich), and 10% FBS, under oil at 5 to 7.5 μL medium/embryo with 2–4 embryos per droplet, and cultured under the same atmosphere.

Blastocyst development was evaluated on days 7 through 10. Embryos showing organization of an outer presumptive trophoblast layer with decreasing density of inner cells were selected as blastocysts. Presumptive blastocysts were fixed in buffered formol saline, mounted on a slide with one drop of mounting medium containing DAPI (Slowfade Diamond Antifade; Invitrogen), and examined using a fluorescence microscope (Axiovert) to determine the number of nuclei. Embryos were classified as blastocysts if they contained ≥ 64 nuclei and had started organization of an outer presumptive trophoblast layer.

Blastocyst nucleus number (number of normal-appearing nuclei) was determined using the cell count feature of ImageJ software (v. 1.48; <https://imagej.nih.gov/ij/>) on photomicrographs of DAPI-stained blastocysts ($n = 19$ and 23 for Conv and Piezo, respectively). Fragmented nuclei or pyknotic nuclei (showing one, or several clustered, small areas of dense chromatin) were counted separately, and the nuclear fragmentation rate (fragmented + pyknotic nuclei/total nuclei) was determined for each embryo.

Culture for evaluation of post-injection kinetics

For evaluation of post-injection kinetics, as noted above, oocytes (three to four per dish) were subjected to Conv or Piezo ICSI, or to Sham-Conv or Sham-Piezo injection, or were placed in the ICSI dish but not injected (Uninj groups). Uninj oocytes were fixed either immediately after the ICSI session was completed (Uninj 0H) or were cultured in M199 with Earle's salts and 10% FBS at 5% CO₂ in air and 38.2 °C for 18 h after the injection session, then fixed (Uninj 18H). Sperm-injected and sham-injected oocytes were fixed either immediately after the ICSI/injection session was completed (0H group) or were similarly cultured for 6 or 18 h after injection, then fixed (6H and 18H groups).

Staining procedures for post-injection kinetics

For simplicity in this report, injected oocytes are referred to as “oocytes” regardless of their developmental stage.

Labeling of sperm mitochondria

To evaluate post-ICSI kinetics, sperm mitochondria were labeled by addition of Mitotracker Red CMXRos (Invitrogen) to the swim-up medium. One microliter of a 1 mM stock solution of the dye in DMSO was added to 1 ml of GMOPS/FBS for a final concentration of 100 μM; this medium was used for the swim-up procedure. The remainder of the sperm preparation and ICSI procedures were performed as described above.

Oocyte fixation and staining

Oocytes were transferred from the ICSI dish or from culture droplets to 4% paraformaldehyde for 20 min, then rinsed in Dulbecco's phosphate-buffered saline (DPBS; Invitrogen) with 2 mg/ml BSA, and held in this medium at 4 °C until staining. PNA, which binds specifically to β-D-galactose moieties, was used to visualize the sperm acrosome and CG; PNA stains both CG contents [37] and the outer acrosomal membrane [38]. For PNA staining, the oocytes were transferred to 0.1% Triton-X 100 in DPBS and held at room temperature for 5 min. Oocytes were washed in DPBS with BSA (2 mg/ml), then placed in a solution of 20 μg/ml PNA in DPBS, and incubated for 30 min in a humidified atmosphere at 37 °C. After incubation, the oocytes were washed in DPBS with BSA.

The oocytes were then placed on a slide (one oocyte per slide) with the minimum medium possible, and allowed to dry approximately 2 min. A 10-μl droplet of the DAPI mounting medium was placed over the oocyte, and the preparation was carefully covered with a glass coverslip. After 10 min, the coverslip was secured by brushing nail polish around the edges. The slides were read at × 400 on an inverted

fluorescence microscope (Axiovert) and on a confocal laser scanning microscope (LSM 780, Zeiss) within 2 days of staining. For the latter, photomicrographs were obtained at the level showing the largest area of sperm chromatin, and at the levels showing clearest red fluorescence indicating the sperm tail and green fluorescence indicating the acrosome.

Classification of sperm and oocyte parameters

Area of sperm chromatin

In sperm-injected oocytes, the area of the sperm head, decondensing chromatin, or male pronucleus (PN) was designated the sperm chromatin area (SCA). The SCA was measured on photographs taken on the inverted microscope, to ensure that the entire chromatin mass was visualized. Images were obtained at a set magnification and resolution. The area in arbitrary units (pixels) was determined by outlining the chromatin using ImageJ software. In mid to late PNs, chromatin aggregated on the side of the male PN that was approaching the female PN, thus the entire circumference was not fluorescent; in this case, the presumptive circumference of the PN, as suggested by the curvature of the visible chromatin, was outlined. The recorded SCA was compared between ICSI treatments at each time period after ICSI, and within treatments over time.

Sperm acrosome and tail

The acrosome was visualized on confocal images or on photographs taken on the inverted microscope as a U-shaped area of green fluorescence typically accompanied by spots within the “U,” and so could be recognized both when on the sperm and when detached. Initially, we classified the acrosome according to intensity and distribution of fluorescence; however, observed differences were minor and this was abandoned. The location of the acrosome was classified as attached to the sperm head or chromatin, separate from the sperm and visible in the oocyte cytoplasm, or not visible.

The tail was visualized due to its red fluorescence. When visible, it was classified as either attached to or detached from the sperm chromatin.

Cortical granules

The cortical granules (CG) were identified as punctate areas of green fluorescence at the periphery of the oocyte, and were classified according to frequency and pattern of staining as prominent, moderate, or trace.

Oocyte chromatin stage

Oocytes were classified based on chromatin configuration, in photographs taken on the inverted microscope, as (1)

metaphase II (MII), chromosomes aligned on a metaphase plate, with first polar body; (2) anaphase to telophase II (AII-TII), two adjacent masses of condensed chromosomes with a first polar body; (3) early pronucleus (PNE), circular area of decondensing chromatin showing textured fluorescence and separate from the male chromatin; (4) mid pronucleus (PNM), larger area of homogenous fluorescence still separate from the male chromatin, with chromatin aggregating to one side of the presumptive circular PN; (5) late pronucleus (PNL), chromatin aggregated to one side of a presumptive circular PN and in contact with the male PN; or (6) first mitotic metaphase to telophase (MIT).

Presence of cytoplasmic extrusions

Masses of apparent cytoplasm separate from the oocyte, within the perivitelline space, and were classified as present or none.

Statistical analysis

Ordinal and nominal categorical data (differences in cleavage and blastocyst rates, and, in the kinetics experiment, in proportion of oocytes showing the different classifications for each measured parameter) were compared using Fisher's exact test. Continuous and non-categorical discrete numerical data were tested for normality using the Shapiro-Wilk test, and non-parametric statistics used if the data were not normally distributed. Data for blastocyst nucleus number was compared between culture days within treatment by ANOVA, and between treatments for all days combined by a one-tailed Student's *t* test, under our original hypothesis of higher embryo quality with Piezo. The nuclear fragmentation rate was compared between culture days within treatment, and between treatments, using the Mann-Whitney *U* test. Sperm head areas were compared between treatments and time periods using the Kruskal-Wallis test with the Dunn post-hoc test. For comparison of post-injection sperm and oocyte parameters between treatments and time periods, in sperm-injected oocytes, only those showing evidence of fertilization, with chromatin that could be placed in the stated classifications, were included in the analyses. Oocytes showing abnormal or atypical chromatin configurations were not included in the analysis. Values were considered significant when $P < 0.05$.

Results

Blastocyst formation after conventional and Piezo ICSI

A total of 169 oocytes were injected for this part of the study; 82 by Conv ICSI and 87 by Piezo ICSI. Cleavage and

blastocyst rates after ICSI with the two techniques are shown in Table 1. There were no significant differences in cleavage rates (89% Conv vs. 87% Piezo) or blastocyst development rates (39% Conv vs. 40% Piezo) between the two techniques ($P > 0.1$). In the Conv treatment, 63% of blastocysts (20/32) were identified on days 7 (12/32) and 8 (8/32) of culture; for Piezo, this proportion was 74% (26/35; 20 day-7 and 6 day-8). This difference was not statistically significant ($P > 0.05$). All blastocysts were identified under light microscopy and verified by DAPI staining (Fig. 1).

There was no significant difference in blastocyst nucleus number (number of normal nuclei) among days within treatment ($P > 0.1$), thus all days were combined. The blastocyst nucleus number was significantly lower for Conv (115 ± 9 , mean \pm s.e.) than for Piezo (140 ± 12 ; $P < 0.05$). The nuclear fragmentation rates did not differ significantly among culture days within treatment ($P > 0.05$). For all days combined, nuclear fragmentation rates were significantly higher in Conv (median 8.4%, range 2.9 to 19.8%) than in Piezo (median 2.2%, range 1.2 to 7.7%; $P < 0.0001$).

Comparison of kinetics of sperm processing and oocyte activation

A total of 250 oocytes were utilized in the morphokinetics study. Of these, 110 oocytes were used for Sham and Uninj treatments; all of these oocytes were analyzable and none were classified as abnormal. Of 140 oocytes that were fixed and stained after ICSI, 6 oocytes were lost during processing, or could not be imaged properly due to mounting issues. Of the 134 oocytes evaluated after ICSI, 4 (3%) were classified as not fertilized (total absence of sperm components; 3 Conv and 1 Piezo). Seven sperm-injected oocytes (5%) were classified as abnormal: two were considered to be degenerated (had shrunken cytoplasm and lacked plasma membrane integrity), three had multiple PNs or multiple aggregations of chromatin, one had a sperm tail visible but no evidence of sperm chromatin, and one had two sperm visible. These oocytes were not included in the analysis; thus, 123 sperm-injected oocytes were analyzed after staining: 62 Conv and 61 Piezo. For any given parameter, some images were not analyzable; thus the *n* varied slightly among parameters and is given in the respective figures and tables.

Confocal images of representative stained oocytes are presented in Fig. 2.

Sperm chromatin area

The change in SCA over time after ICSI in the two treatments is presented in Fig. 3a. At 0H, there was no difference in median SCA between treatments (1289 and 1210 for Conv and Piezo, respectively). Confocal images of sperm in different stages of decondensation are presented in Fig. 4. On evaluation under confocal microscopy, all sperm at 0H showed a

Table 1 Cleavage and blastocyst rates after conventional or Piezo-driven ICSI

Treatment	Oocytes injected <i>n</i>	Oocytes cleaved (%)	Blastocysts (%)	Day 7–8 blastocysts (%)
Conventional	82	73/82 (89%)	32/82 (39%)	20/32 (63%)
Piezo	87	76/87 (87%)	35/87 (40%)	26/35 (74%)

There were no significant differences in cleavage rate, blastocyst rate, or proportion of blastocysts developing on days 7 and 8, vs. days 9 and 10, after ICSI between the two treatments ($P > 0.1$)

smooth sperm head outline, with the exception of three sperm (1/17 Conv, 2/16 Piezo) in which an irregular protrusion of chromatin was visible on one side of the post-acrosomal region, indicating initiation of chromatin decondensation (Fig. 4b).

At 6H, the sperm chromatin in the majority of oocytes (74%, 14/19) in the Conv treatment remained condensed (were within $1.5 \times$ the inter-quartile range of the 0H median area). There was no significant difference in median SCA between 0H and 6H for Conv. In contrast, in Piezo oocytes at 6H, only 15% (3/20) still showed condensed sperm chromatin; the median SCA in the Piezo treatment increased significantly between 0H and 6H ($P < 0.001$). At 6H, the median SCA was significantly lower for Conv than for Piezo (1340 vs. 4079, respectively; $P < 0.05$).

The median SCA increased significantly between 6H and 18H for Conv ($P < 0.001$) and tended to increase for Piezo ($P = 0.07$). There was no significant difference in median

SCA between treatments at 18H (62,328 and 72,953 for Conv and Piezo, respectively; $P > 0.1$).

Seven oocytes (three Conv and four Piezo) had progressed to metaphase or anaphase of the first mitotic division at 18H; these oocytes were not included in the SCA calculations at 18H.

Sperm acrosome and tail

The proportion of oocytes showing the different categories of acrosome status is presented in Fig. 3b. At 0H, the acrosome was visible on the sperm inside the oocyte (Figs. 2c, d and 4a) in 76.5% (13/17) of Conv and 100% (16/16) of Piezo oocytes; in an additional oocyte (5.9%) in the Conv treatment at 0H, the acrosome was detached from the sperm head and visible in the oocyte cytoplasm (Figs. 2f, g and 4d). Between 0H and 6H, the percentage of injected oocytes showing sperm with intact acrosomes did not change significantly in Conv, but

Fig. 1 Blastocysts produced after ICSI with conventional (a brightfield; b DAPI) and Piezo (c brightfield; d DAPI) techniques. All blastocysts in this study were verified on DAPI staining. Bar = 50 μ m

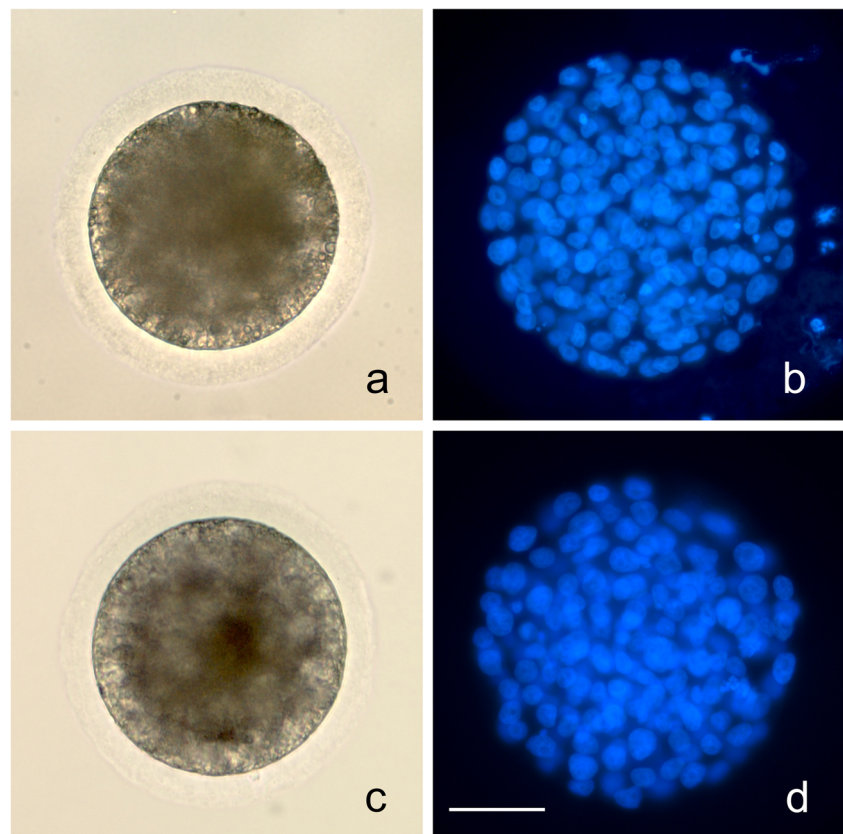
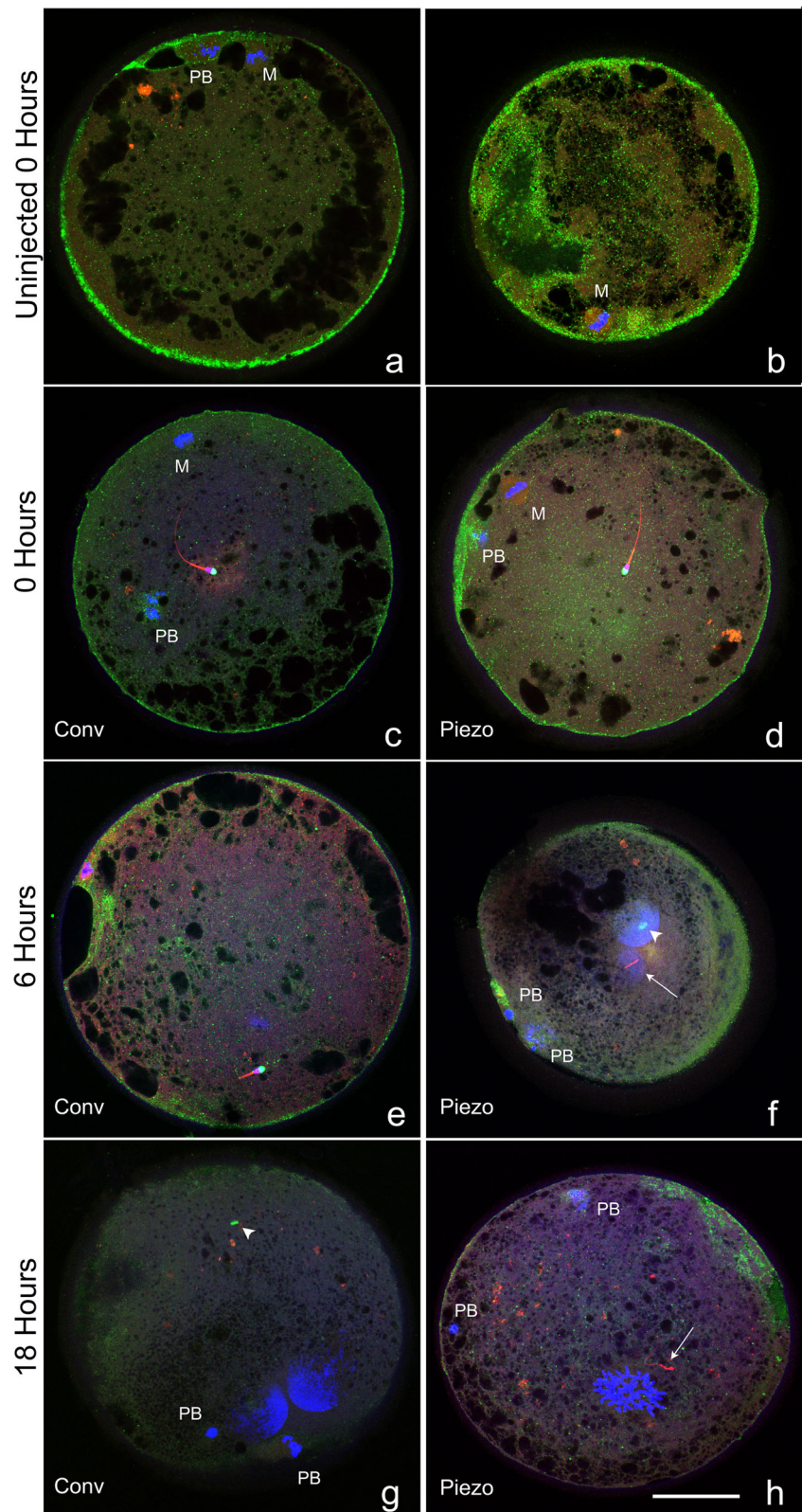


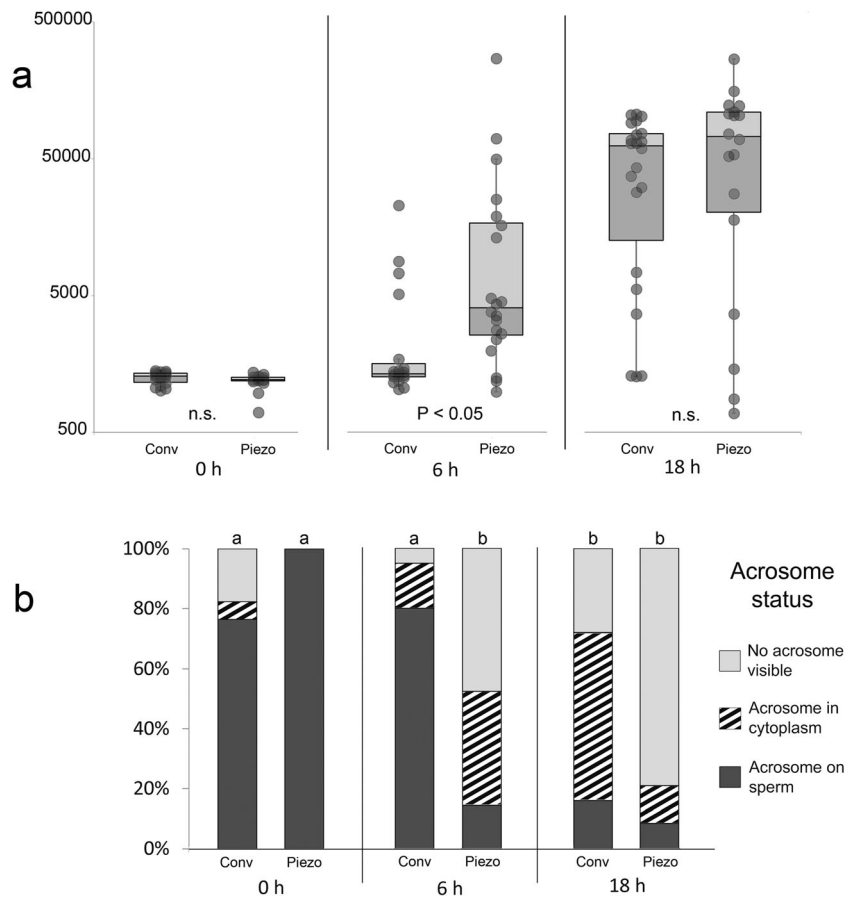
Fig. 2 Confocal images of oocytes that were uninjected, or at 0, 6, or 18 h after conventional or Piezo ICSI, demonstrating different classifications of chromatin (DAPI, blue), acrosome (PNA, green), tail (MitoTracker Red CMXRos, red), and cortical granules (PNA, green). **a–e** MII oocytes (where visible; *M* oocyte metaphase plate, *PB* first polar body) each demonstrating a central sperm with intact sperm tail and acrosome. **f, g** Oocytes demonstrating two mid-stage pronuclei (large blue masses) and two polar bodies (PB), the acrosome is visible in the cytoplasm (arrowhead, green). The sperm tail is visible in (**f**) (arrow), and was present in the cytoplasm of (**g**) but is not visible in this focal plane. **h** Oocyte in prometaphase of the first mitotic division (blue area toward 6:00), with two polar bodies (PB). Sperm tail is visible in cytoplasm (arrow), no acrosome was visualized. Cortical granules were classified as prominent (**a, b**), moderate (**c–e**), and trace (**f–h**). Bar = 50 μ m



decreased significantly in Piezo; thus, at 6H, the proportion of oocytes having sperm with detached acrosomes was significantly higher in Piezo (86%, 18/21 vs. 20%, 4/20 for Conv;

$P < 0.0001$). Moreover, the proportion of oocytes that still showed a visible acrosome, either attached to the sperm head or in the cytoplasm, was significantly higher in Conv than in

Fig. 3 a Whisker plot showing median, 1st and 3rd quartile of relative sperm chromatin areas at 0, 6, and 18 h after Conventional or Piezo ICSI. Chromatin area for each sperm is represented as a dot; error bars represent $1.5 \times$ the interquartile range. Note logarithmic scale on Y axis. Values with different superscripts differ significantly ($P < 0.05$). **b** Proportion of oocytes showing the different acrosome classifications at 0, 6, and 18 h after Conventional or Piezo ICSI. ^{a,b}Values for *Acrosome on sperm* differ significantly ($P < 0.001$)



Piezo at both 6H (95%, 19/20 vs. 52%, 11/21, respectively; $P < 0.01$) and 18H (72%, 18/25 vs. 21%, 5/24, respectively; $P < 0.001$). At 18H, the acrosome was still present on the sperm chromatin in 16% of Conv and 8% of Piezo oocytes, and could even be seen on sperm chromatin that had progressed to the PN stage (Fig 4e).

The sperm tail was visible in all injected oocytes at every time period, with the exception of three oocytes at 18H (1/24 Conv and 2/22 Piezo); all of the latter were in mid- to late-PN stages. For oocytes in which the sperm tail was visible, the proportion of tails attached to the sperm chromatin varied significantly among time periods. At 0H, 100% of sperm tails were attached to the sperm chromatin in both treatments. The proportion of attached tails decreased significantly between 0H and 6H within both treatments (to 75%, 15/20 for Conv, $P < 0.05$ and to 29%, 6/21 for Piezo, $P < 0.0001$), but at 6H was significantly higher for Conv than for Piezo ($P < 0.01$). The proportion of attached tails decreased significantly between 6H and 18H in the Conv treatment (to 22%, 5/23, $P < 0.001$) but not in the Piezo (6/20, 30%, $P > 0.05$). Of the 11 oocytes that still had the sperm tails apparently attached to the sperm chromatin at 18H, 6 (3/20 Conv and 3/23 Piezo) were associated with sperm showing no to minimal chromatin decondensation at that time; however, in the other five (2/20 Conv and 3/23 Piezo), the sperm chromatin had progressed to

the PN stage and the sperm tail was visible apparently attached to the PN chromatin, in the same confocal plane (Fig. 4e).

Oocyte activation

Representative images of oocytes in the different oocyte chromatin stages are presented in Fig. 5, and the meiotic or developmental stage of the oocyte chromatin at the different time periods is presented in Table 2. All Uninj oocytes were at MII at both 0H and 18H. Of 78 Sham-injected oocytes, 74 were at MII. One oocyte at 0H and one at 6H (both Sham-Conv) were at AII-TII, and two at 18H (Sham-Piezo) were at PNL. All sperm-injected oocytes at 0H were at MII, except for one oocyte in Conv that had progressed to AII-TII. At 6H, a significantly higher proportion of oocytes in the Conv treatment were still in MII (80%, 16/20 vs. 9.5%, 2/21 for Piezo; $P < 0.0001$). Of the 16 oocytes still at MII in the Conv treatment at 6H, 12 were associated with apparent intact condensed sperm chromatin, and 4 had sperm with some evidence of decondensation. A similar proportion of oocytes had progressed to the PN or MIT stage at 18H in the two treatments (76%, 19/25 for Conv and 75%, 18/24 for Piezo, $P > 0.1$); however, the proportion of these oocytes showing late PN to MIT vs. early or mid-stage PN was significantly

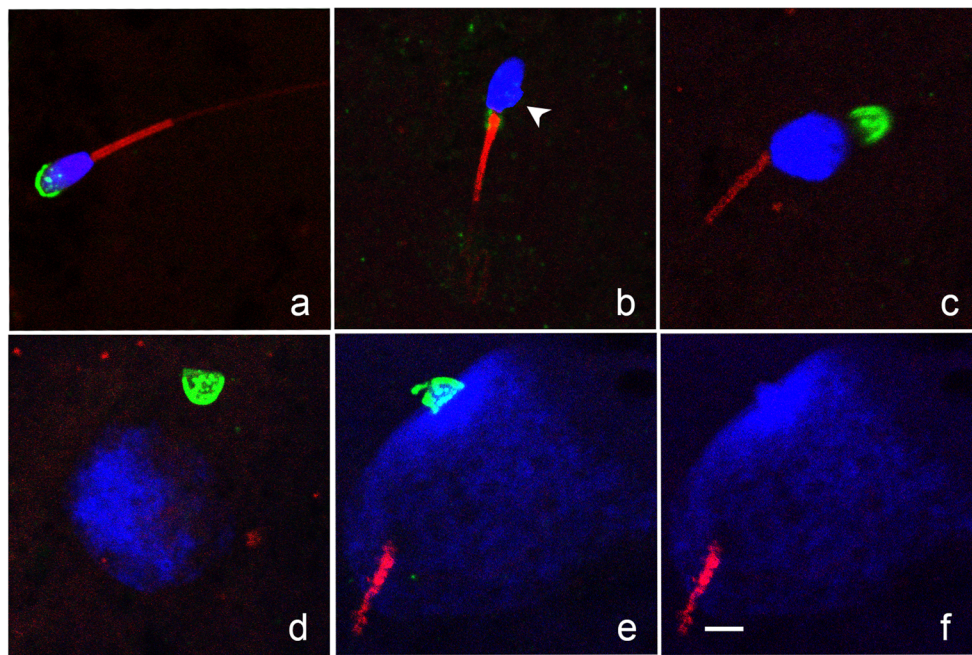


Fig. 4 Confocal images of sperm chromatin (DAPI, blue), acrosome (PNA, green), and tail (MitoTracker Red CMXRos, red) showing different configurations. **a** Condensed sperm head with intact acrosome and tail. **b** Sperm head showing initial signs of decondensation (irregular protrusion of chromatin at base of head; arrowhead). Sperm tail is intact; acrosome was not visualized. We noted that remnants of the proximal droplet stained with PNA (green fluorescence on the midpiece at the

junction of the sperm head and tail). **c** decondensing sperm chromatin, intact tail, and detached acrosome. **d** Early pronucleus with detached acrosome. **e, f** Mid-pronucleus with adjacent sperm tail; acrosome remained intact and chromatin within the acrosome failed to decondense, the green channel is removed in (**f**) to demonstrate chromatin clearly. Bar = 5 μ m

lower in Conv than Piezo (42%, 8/19 vs. 83%, 15/18, respectively; $P < 0.05$).

The status of CG at the periphery of the oocyte in the different groups is presented in Fig. 6. At 0H, the proportion of oocytes with prominent CG (Fig. 2a, b) was significantly lower in all injected groups than in Uninj oocytes ($P < 0.01$). Loss of CG (to trace) was seen in some injected oocytes at 0H. The proportion of oocytes with trace CG increased significantly over time in Piezo (0H vs. 6H, $P < 0.01$; 0H vs. 18H, $P < 0.001$), and tended to increase over time in Conv (0 vs. 18H, $P = 0.08$). In sperm-injected oocytes, the proportion of oocytes having prominent CG decreased non-significantly over time. In contrast, in sham-injected groups, the proportion of oocytes with prominent CG tended to increase, and the proportion of oocytes with trace CG tended to decrease over time. At 18H, there was no significant difference in trace CG between the Sham treatments and Uninj 18H ($P > 0.1$), whereas in sperm-injected oocytes at 18H, the proportion of oocytes with trace CG was significantly higher in Piezo than in Uninj 18H ($P < 0.01$) and tended to be higher in Conv than in Uninj 18H ($P = 0.08$).

The presence of cytoplasmic extrusions in the perivitelline space was seen only at 18H, in a total of 11 sperm-injected oocytes (6/25, 24% of Conv and 5/24, 21% of Piezo; $P > 0.1$). Of these 11 oocytes, 9 (4 Conv and 5 Piezo) were in mid to late PN or MIT stages. The extrusions tended to be associated

with PNA-staining granules (Fig. 7c). In two of the nine oocytes, a comma-shaped deformation of the oocyte was observed at the plane of the confocal image, with the tip of the deformation associated with the extrusions. We designated this projection from the oocyte the “extrusion cone,” as it appeared to lead to the extrusions. On further evaluation of confocal images of all PNM to MIT oocytes, two additional oocytes, both PNM, displayed an extrusion cone but no extrusions. We observed that in all cases, the cone was in close proximity to a polar body (Fig. 7a–c).

Discussion

To the best of our knowledge, this is the first report comparing sperm component remodeling and oocyte activation after fertilization via ICSI with two techniques in a validated system. The results of this study show that the kinetics of development within the first 18 h after fertilization, including oocyte activation and processing of both sperm chromatin and acrosome, differ significantly depending on the method used for sperm immobilization and injection. The delay in activation in the Conv treatment suggests a slower release of sperm factors, which is consistent with a more limited disruption of the sperm plasma membrane after immobilization and injection with this technique. This is the first study to report that the

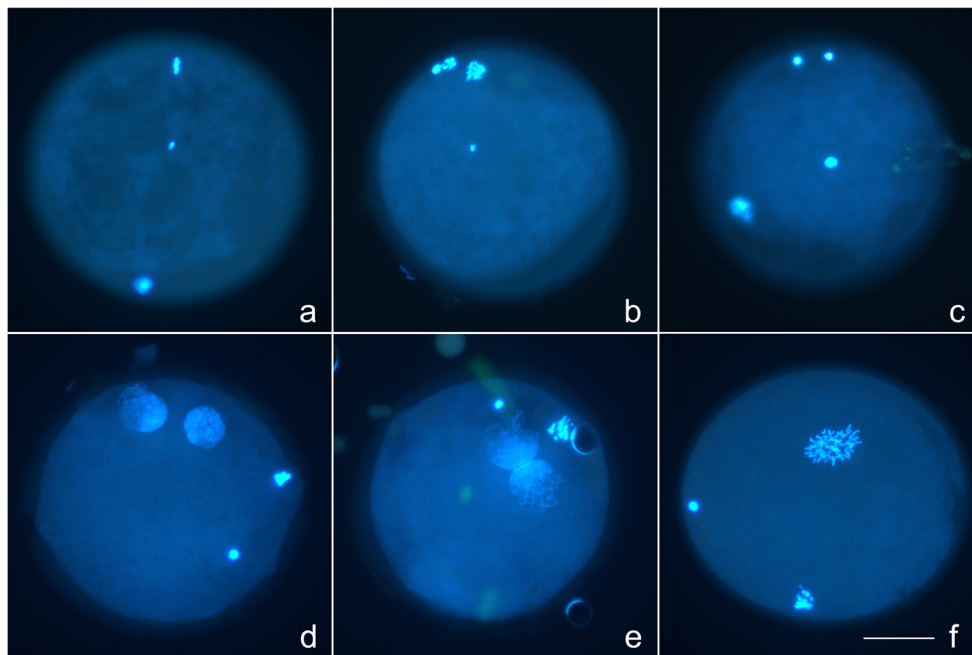


Fig. 5 Photomicrographs taken on the inverted fluorescent microscope, demonstrating stages of oocyte activation and sperm head decondensation. **a** Metaphase II oocyte (metaphase plate at 12:00 and first polar body at 6:00) with central condensed sperm head. **b** Anaphase II with first polar body at 11:00, showing signs of division, and separating anaphase chromosomes at 12:00, with central condensed sperm head. **c** Telophase II with two masses of oocyte chromatin at 12:00

and first polar body at 8:00, with central decondensing sperm head. **d** Early pronuclear-stage oocyte with pronuclei at 12:00 and 1:00, and two polar bodies (3:00 and 4:00). **e** Late pronuclear-stage oocyte with pronuclei in contact with one another, and two polar bodies (12:00 and 2:00). **f** Oocyte in prometaphase of first mitosis, with two polar bodies (6:00 and 9:00). Note apparent cytoplasmic extrusion cone in perivitelline space between 2:00 and 3:00. Bar = 50 μ m

two techniques provide similar high blastocyst rates (39 and 40% for Conv and Piezo, respectively) after ICSI in the horse. It is notable that the blastocyst development in the Piezo

treatment was achieved using a non-toxic fluorocarbon-based fluid as ballast, which supports the evaluation of this technique for use in human-assisted reproduction settings. Some

Table 2 Chromatin stage of oocytes that were uninjected, or at 0, 6, or 18 h after conventional or Piezo ICSI or sham injection.

Treatment	Time period	n	Oocyte stage n (%)					
			MII	AII-TII	PNE	PNM	PNL	MIT
Uninjected	0H	11	11 (100.0)					
	18H	21	21 (100.0) ^c					
Conventional	0H	17	16 (94.1)	1 (5.9)				
	6H	20	16 (80.0) ^a	3 (15.0)	1 (5.0)			
	18H	25	2 (8.0) ^d	4 (16.0)	3 (12.0)	8 (32.0)	5 (20.0)	3 (12.0)
Piezo	0H	16	16 (100.0)					
	6H	21	2 (9.5) ^b	13 (61.9)	4 (19.1)	2 (9.5)		
	18H	24	3 (12.5) ^d	3 (12.5)	1 (4.2)	2 (8.3)	11 (45.8)	4 (16.7)
Sham-Conv	0H	12	11 (91.7)					
	6H	14	13 (92.9) ^a	1 (7.1)				
	18H	13	13 (100.0) ^c					
Sham-Piezo	0H	13	13 (100.0)					
	6H	13	13 (100.0) ^a					
	18H	13	11 (84.6) ^c					
							2 (15.4)	

Within time period (^{a,b} 6H, ^{c,d} 18H) proportions of oocytes at MII with different superscripts differ significantly ($P < 0.0001$). There were no significant differences at 0H

MII metaphase II, AII-TII anaphase II to telophase II, PNE early pronucleus, PNM mid pronucleus, PNL late pronucleus, MIT first mitosis

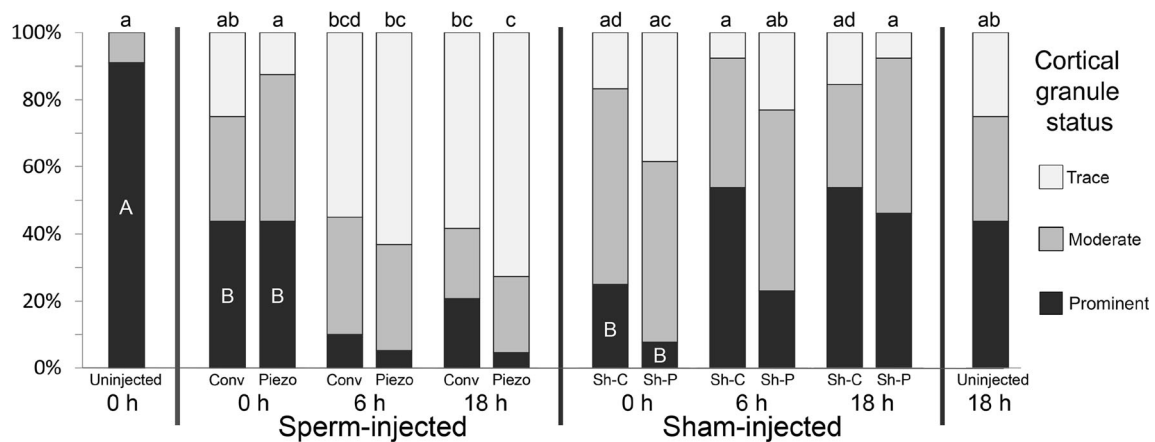


Fig. 6 Proportion of oocytes showing prominent, moderate, or trace cortical granules (CG) at the periphery of the cytoplasm in uninjected oocytes at 0 or 18 h, and at 0, 6, and 18 h after conventional (Conv) and Piezo ICSI or sham injection (Sh-C and Sh-P, respectively). ^{a-d} For

Trace CG, values with different superscripts differ significantly ($P < 0.05$); A, B: For Prominent CG, within 0H groups, values with different letters differ significantly ($P < 0.01$)

caveats apply to interpretation of the findings of the study; the work was done with fertile research animals, and results could differ in a clinical setting with subfertile animals. In addition, the oocytes in this study were recovered from immature follicles and matured in vitro; it is possible that in vivo-matured oocytes aspirated from stimulated preovulatory follicles, as is standard procedure in humans, could better process sperm after ICSI with the conventional technique. In a recent report, no significant differences were found in the kinetics of development after ICSI, using the Piezo, between in vivo- and in vitro-matured equine oocytes [39]; however, the number of oocytes compared was low.

In human ART, time-lapse imaging has suggested that the kinetics of early development can predict embryo quality, even in embryos that have similar morphology on the day of selection [review, 40]. In our study, the nucleus number was lower in Conv- than in Piezo-produced blastocysts, the nuclear fragmentation rate was higher, and there was a tendency for

later blastocyst development. These data indicate that the differences observed in developmental kinetics in the 18H after sperm injection in the Conv treatment were associated with lower blastocyst quality. This reflects findings after conventional and Piezo ICSI in the pig, which suggested that the developmental kinetics after Piezo ICSI may more closely resemble those after standard IVF [8]. There is little information available on measures of embryo quality in in vitro-produced (IVP) equine blastocysts. The present study is one of the first to use nucleus number and nuclear fragmentation rate as a measure of quality in these embryos. We have recently developed the protocol used in this study for assessing nuclear fragmentation, and have validated it by comparing the observed nuclear fragmentation rate with the percentage of TUNEL-positive nuclei, in vitrified-warmed equine IVP blastocysts ($n = 34$). The percentage of fragmented nuclei on evaluation of DAPI-stained embryos was strongly correlated ($r = 0.86$; $P < 0.0001$) with the proportion of apoptotic nuclei

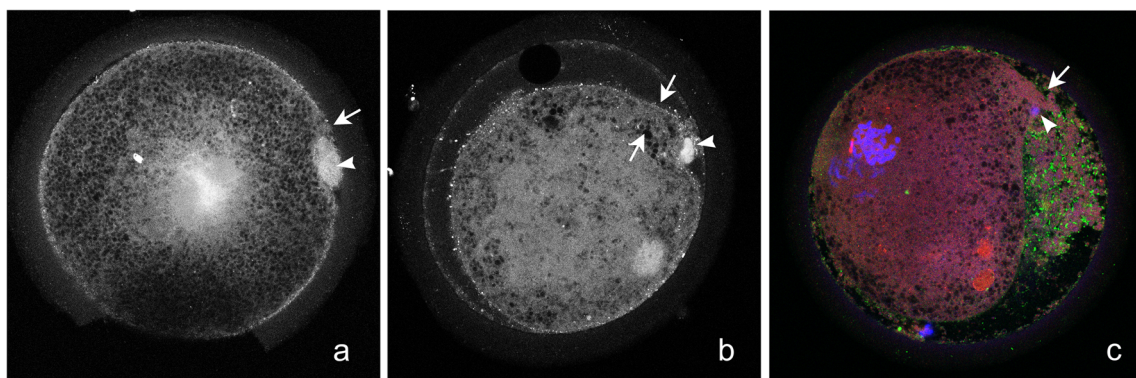


Fig. 7 Confocal images of oocytes at 18 h after ICSI, showing presence of a protrusion from the oocyte (“extrusion cone,” arrow) in the area of a polar body (arrowhead). The extrusion cone was associated with presence

of cytoplasmic extrusions in the perivitelline space (b, c). The cytoplasmic extrusions tended to have accumulations of PNA-positive granules (c)

as determined by TUNEL staining (unpublished data). Unfortunately, there is essentially no information available on the relationship of different measures of IVP equine blastocyst quality to pregnancy status after embryo transfer to recipient mares.

In human sperm, there is conflicting data on acrosome status after immobilization. Evaluation of human sperm via scanning electron microscopy after conventional immobilization showed apparent acrosomal disruption in 96% of manipulated sperm in one study [41], whereas other researchers using transmission electron microscopy found that only 17% of immobilized sperm showed acrosomal loss [42]. In the sheep, 46% of sperm underwent acrosomal disruption after Piezo immobilization vs. 20% of non-manipulated sperm [9]. We hypothesized that use of the Piezo drill would result in acrosomal loss before sperm injection; however, we found that the acrosome was visualized intact on 100% of sperm at 0H after Piezo ICSI. As Piezo ICSI in our study led to a 40% blastocyst rate, these data clearly demonstrate that in the horse, embryonic development to the blastocyst stage can occur after injection of sperm having intact acrosomes. We found that when the acrosome detached from the sperm after ICSI, it was shed almost intact into the cytoplasm, similar to the fate of the perinuclear theca as reported after conventional ICSI in rhesus [43]. This contrasts with the findings reported in the pig and human, in which the acrosome underwent the acrosome reaction or gradually disintegrated after conventional ICSI [44–46]. We observed that persistence of the acrosome visibly affected the decondensation of the underlying chromatin in some oocytes (Fig. 4F), as reported previously after ICSI in rhesus [43, 47]. This phenomenon may affect the synchrony of sperm chromatin processing and possibly lead to detrimental effects on embryo quality. Our data suggests that delayed acrosomal loss and aberrant chromatin decondensation are more likely to occur when ICSI is performed using the conventional technique.

Remarkably, the beginning of sperm chromatin decondensation, i.e., protrusion of an irregular chromatin mass at the base of the head, was seen in one Conv and two Piezo oocytes evaluated at 0H (3/35, 9%), suggesting rapid initiation of developmental events after ICSI. Other indicators of rapid oocyte activation were seen in injected oocytes at 0H, i.e., significant loss of cortical granule-associated fluorescence and presence of two oocytes already at AII–TII at the time of evaluation. While these oocytes were designated as 0H, three to four oocytes were placed in the same dish for micromanipulation, so the actual time from injection to fixation varied from 1 to ~15 min, according to the order in which injection was performed on oocytes in that dish.

At 6H, the significant difference in median sperm head area between Conv and Piezo (Fig. 3a) demonstrated clearly that sperm chromatin processing is not equivalent after ICSI with these two techniques in the horse. This is similar to findings in

the pig 10 to 12 h after sperm injection with conventional vs. Piezo ICSI [8]. Reflecting this difference in sperm chromatin processing, we found that oocyte progression from MII at 6H was significantly lower in Conv than in Piezo. Progression from MII was dependent upon sperm injection, as 24/26 (92%) of sham-injected oocytes remained at MII at 18 h, vs. 5/49 (10%) of sperm-injected oocytes. Our data on oocyte meiotic progression in the Piezo treatment agree with those of Ruggeri et al. [39], using the Piezo, who reported that 5/6 normally fertilized IVM oocytes had progressed from MII at 6H, and 7/7 were in the PN stage at 16H. Our findings for the Conv treatment appear to conflict with those of Tremoleda et al. [30], who described chromatin and cytoskeletal morphology in equine oocytes after conventional ICSI. These authors reported that 75% of successfully injected oocytes showed signs of activation at 6 h. However, in that study, signs of activation included findings such as enlargement of chromosomes in MII oocytes; the actual meiotic stage of the oocytes was not detailed. In our study, we classified each oocyte by meiotic stage and considered all MII oocytes to be non-activated.

We found that the sperm tail was present in essentially every injected oocyte examined. The tails were attached to sperm at 0H, but the majority of tails had detached from the sperm by 6H in Piezo and by 18H in Conv. The sperm tail is incorporated into the oocyte after fertilization in vivo in the horse [48], thus its presence should be compatible with normal embryo development.

We were surprised to find a significant reduction in CG prominence in oocytes fixed immediately after ICSI (0H), in both Conv and Piezo treatments, when compared to Uninj 0H oocytes (44 and 44% vs. 91% with prominent CG, respectively). Since the injected oocytes were fixed 1 to 15 min after ICSI, this suggests that the cortical reaction is rapidly induced after the injection procedure. Oocytes subjected to sham injection also showed low proportions of prominent CG at 0H (25 and 8% for Conv and Piezo sham injection, respectively), thus this CG loss appears to be related to the injection procedure itself, rather than to a rapid release of oocyte-activating factors from sperm. The injection procedure involves both disruption of the oolemma and influx of external medium. While there could be some effect of mechanical disruption of the oolemma on CG release, the most likely mechanism is a massive calcium influx into the oocyte associated with injection. Cortical granule exocytosis is mediated by calcium, via a pathway that is not yet completely understood [49–51]. Both the injection medium and the oocyte holding medium (which may enter into the oocyte as the plasma membrane is broken) contain millimolar concentrations of calcium (~2 mM (D. Rieger, LifeGlobal, personal communication 2018) for injection medium and 1.3 mM for holding medium). This is in contrast to the nanomolar intracellular calcium concentrations in resting oocytes [52]; thus,

it is likely that this influx of calcium associated with injection triggers CG loss.

Interestingly, a decrease in CG prominence (to trace) was seen at 6H in both sperm-injected treatments; in contrast, in sham-injected oocytes, the proportion of prominent CG actually tended to increase over time. This suggests that further CG loss after ICSI is triggered by sperm-related factors, likely by release and action of the putative sperm factor PLC ζ [53], which has been described in equine sperm [54], and induces recurring calcium oscillations [55]. Cortical granule formation and translocation to the periphery is a continuous process (review [50]), thus the tendency for CG recrudescence seen in sham-injected oocytes over time may be due to the absence of a continued activation stimulus (calcium signaling) after the initial injection.

We noted the presence of cytoplasmic extrusions from the zygote at 18H, associated with the most advanced stages of development. The extrusions were present in 1/9 (11%) sperm-injected oocytes in the mid-PN stage, and in 8/19 (42%) sperm-injected oocytes in the late PN or first mitosis stages. We have noted these extrusions commonly when evaluating early IVP equine embryos. The cytoplasmic extrusions are not an artifact of the ICSI procedure, as they are seen in early horse embryos fertilized in vivo [56–58], and via standard IVF [57], including in an embryo known to have produced a foal [59]. The extrusions do not seem to represent blastomere fragmentation, as they occur before cleavage is initiated, as seen in the present study. On further evaluation of images of oocytes at 18H to try to characterize the extrusions, we observed a deformation (extrusion cone) in some oocytes, as detailed in the “Results” section. We hypothesize that the oocyte actively extrudes cytoplasm through this structure before the onset of the first cleavage. The reason for this phenomenon is unclear; however, we also consistently observed an accumulation of PNA-positive granules among the extrusions, so it is possible that the oocyte is discarding selected cytoplasmic components.

In conclusion, we report the differential kinetics of early developmental events after conventional and Piezo ICSI, in a validated model responsive to both techniques. A significant delay in onset of sperm chromatin decondensation, acrosomal loss, and oocyte meiotic resumption was found after conventional ICSI. These findings suggest a slower release of sperm factors, consistent with a more limited disruption of the plasma membrane, after conventional immobilization and injection. The delay in activation was associated with lower embryo quality at the blastocyst stage, despite equivalent blastocyst rates between treatments. If similar differences between micromanipulation techniques occur in human ICSI, it is possible that use of the Piezo may help to improve embryo quality. The possibility that a simple change in ICSI technique may improve IVF cycle outcome warrants further investigation.

Acknowledgements We thank Ms. Kindra Rader and Dr. Josefina Kjollerstrom for excellent technical assistance, and Dr. Roula Barhoumi Mounaime for invaluable assistance with confocal microscopy.

Compliance with ethical standards

Conflict of interest The authors declare that they have no conflict of interest.

References

1. Sherins RJ, Thorsell LP, Dorfmann A, Dennison-Lagos L, Calvo LP, Krysa L, et al. Intracytoplasmic sperm injection facilitates fertilization even in the most severe forms of male infertility: pregnancy outcome correlates with maternal age and number of eggs available. *Fertil Steril*. 1995;64:369–75.
2. Salamone DF, Canel NG, Rodriguez MB. Intracytoplasmic sperm injection in domestic and wild mammals. *Reproduction*. 2017;154:F111–f24.
3. Galli C, Duchi R, Colleoni S, Lagutina I, Lazzari G. Ovum pick up, intracytoplasmic sperm injection and somatic cell nuclear transfer in cattle, buffalo and horses: from the research laboratory to clinical practice. *Theriogenology*. 2014;81:138–51.
4. Dyer S, Chambers GM, de Mouzon J, Nygren KG, Zegers-Hochschild F, Mansour R, et al. International Committee for Monitoring Assisted Reproductive Technologies world report: assisted reproductive technology 2008, 2009 and 2010. *Hum Reprod*. 2016;31:1588–609.
5. Schlegel PN, Girardi SK. Clinical review 87: In vitro fertilization for male factor infertility. *J Clin Endocrinol Metab*. 1997;82:709–16.
6. Kimura Y, Yanagimachi R. Intracytoplasmic sperm injection in the mouse. *Biol Reprod*. 1995;52:709–20.
7. Yanagida K, Katayose H, Hirata S, Yazawa H, Hayashi S, Sato A. Influence of sperm immobilization on onset of Ca(2+) oscillations after ICSI. *Hum Reprod*. 2001;16:148–52.
8. Katayama M, Sutovsky P, Yang BS, Cantley T, Rieke A, Farwell R, et al. Increased disruption of sperm plasma membrane at sperm immobilization promotes dissociation of perinuclear theca from sperm chromatin after intracytoplasmic sperm injection in pigs. *Reproduction*. 2005;130:907–16.
9. Anzalone DA, Iuso D, Czernik M, Ptak G, Loi P. Plasma membrane and acrosome loss before ICSI is required for sheep embryonic development. *J Assist Reprod Genet*. 2016;33:757–63.
10. Lacham-Kaplan O, Trounson A. Intracytoplasmic sperm injection in mice: increased fertilization and development to term after induction of the acrosome reaction. *Hum Reprod*. 1995;10:2642–9.
11. Morozumi K, Shikano T, Miyazaki S, Yanagimachi R. Simultaneous removal of sperm plasma membrane and acrosome before intracytoplasmic sperm injection improves oocyte activation/embryonic development. *Proc Natl Acad Sci U S A*. 2006;103:17661–6.
12. Seita Y, Ito J, Kashiwazaki N. Removal of acrosomal membrane from sperm head improves development of rat zygotes derived from intracytoplasmic sperm injection. *J Reprod Dev*. 2009;55:475–9.
13. Zambrano F, Aguila L, Arias ME, Sanchez R, Felmer R. Improved preimplantation development of bovine ICSI embryos generated with spermatozoa pretreated with membrane-destabilizing agents lysolecithin and Triton X-100. *Theriogenology*. 2016;86:1489–97.
14. Yanagida K, Hatayose H, Yazawa H, Kimura Y, Konnai K, Sato A. The usefulness of a piezo-micromanipulator in intracytoplasmic sperm injection in humans. *Hum Reprod*. 1998;14:448–53.

15. Takeuchi S, Minoura H, Shibahara T, Shen X, Futamura N, Toyoda N. Comparison of piezo-assisted micromanipulation with conventional micromanipulation for intracytoplasmic sperm injection into human oocytes. *Gynecol Obstet Investig.* 2001;52:158–62.
16. Hiraoka K, Kitamura S. Clinical efficiency of piezo-ICSI using micropipettes with a wall thickness of 0.625 μm . *J Assist Reprod Genet.* 2015;32:1827–33.
17. Galli C, Vassiliev I, Lagutina I, Galli A, Lazzari G. Bovine embryo development following ICSI: effect of activation, sperm capacitation and pre-treatment with dithiothreitol. *Theriogenology.* 2003;60:1467–80.
18. Garcia-Rosello E, Garcia-Mengual E, Coy P, Alfonso J, Silvestre MA. Intracytoplasmic sperm injection in livestock species: an update. *Reprod Domest Anim.* 2009;44:143–51.
19. Zhou X, Yin M, Jiang W, Jiang M, Li S, Li H, et al. Electrical activation of rabbit oocytes increases fertilization and embryo development by intracytoplasmic sperm injection using sperm from deceased male. *J Assist Reprod Genet.* 2013;30:1605–10.
20. Colleoni S, Barbacini S, Necchi D, Duchi R, Lazzari G, Galli C. Application of ovum pick-up, intracytoplasmic sperm injection and embryo culture in equine practice. *Proc Amer Assoc Equine Pract.* 2007;53:554–9.
21. Hinrichs K, Choi YH, Norris JD, Love LB, Bedford-Guaus SJ, Hartman DL, et al. Evaluation of foal production following intracytoplasmic sperm injection and blastocyst culture of oocytes from ovaries collected immediately before euthanasia or after death of mares under field conditions. *J Am Vet Med Assoc.* 2012;241:1070–4.
22. Hinrichs K, Choi YH, Love CC, Spacek S. Use of intracytoplasmic sperm injection and in vitro culture to the blastocyst stage in a commercial equine assisted reproduction program. *J Equine Vet Sci.* 2014;34:176.
23. Hinrichs K, Choi YH, Love LB, Varner DD, Love CC, Walckenaer BE. Chromatin configuration within the germinal vesicle of horse oocytes: changes post mortem and relationship to meiotic and developmental competence. *Biol Reprod.* 2005;72:1142–50.
24. Galli C, Colleoni S, Duchi R, Lagutina I, Lazzari G. Developmental competence of equine oocytes and embryos obtained by in vitro procedures ranging from in vitro maturation and ICSI to embryo culture, cryopreservation and somatic cell nuclear transfer. *Anim Reprod Sci.* 2007;98:39–55.
25. Altermatt JL, Suh TK, Stokes JE, Carnevale EM. Effects of age and equine follicle-stimulating hormone (eFSH) on collection and viability of equine oocytes assessed by morphology and developmental competency after intracytoplasmic sperm injection (ICSI). *Reprod Fertil Dev.* 2009;21:615–23.
26. Foss R, Ortis H, Hinrichs K. Effect of potential oocyte transport protocols on blastocyst rates after intracytoplasmic sperm injection in the horse. *Equine Vet J.* 2013;45:39–43.
27. Smits K, Govaere J, Hoogewijs M, Piepers S, Van Soom A. A pilot comparison of laser-assisted vs piezo drill ICSI for the in vitro production of horse embryos. *Reprod Domest Anim.* 2012;47:e1–3.
28. Alonso A, Baca Castex C, Ferrante A, Pinto M, Castaneira C, Trasorras V, et al. In vitro equine embryo production using air-dried spermatozoa, with different activation protocols and culture systems. *Andrologia.* 2015;47:387–94.
29. Dini P, Bogado Pascottini O, Ducheyne K, Hostens M, Daels P. Holding equine oocytes in a commercial embryo-holding medium: new perspective on holding temperature and maturation time. *Theriogenology.* 2016;86:1361–8.
30. Tremoleda JL, Van Haefen T, Stout TA, Colenbrander B, Bevers MM. Cytoskeleton and chromatin reorganization in horse oocytes following intracytoplasmic sperm injection: patterns associated with normal and defective fertilization. *Biol Reprod.* 2003;69:186–94.
31. Smits K, Govaere J, Peelman LJ, Goossens K, de Graaf DC, Vercauteren D, et al. Influence of the uterine environment on the development of in vitro-produced equine embryos. *Reproduction.* 2012;143:173–81.
32. Carnevale EM. The mare model for follicular maturation and reproductive aging in the woman. *Theriogenology.* 2008;69:23–30.
33. Ginther OJ. The mare: a 1000-pound guinea pig for study of the ovulatory follicular wave in women. *Theriogenology.* 2012;77:818–28.
34. Jacobson CC, Choi YH, Hayden SS, Hinrichs K. Recovery of mare oocytes on a fixed biweekly schedule, and resulting blastocyst formation after intracytoplasmic sperm injection. *Theriogenology.* 2010;73:1116–26.
35. Choi YH, Love LB, Varner DD, Hinrichs K. Holding immature equine oocytes in the absence of meiotic inhibitors: effect on germinal vesicle chromatin and blastocyst development after intracytoplasmic sperm injection. *Theriogenology.* 2006;66:955–63.
36. Martino NA, Dell'Aquila ME, Filioli Uranio M, Rutigliano L, Nicassio M, Lacalandra GM, et al. Effect of holding equine oocytes in meiosis inhibitor-free medium before in vitro maturation and of holding temperature on meiotic suppression and mitochondrial energy/redox potential. *Reprod Biol Endocrinol.* 2014;12:99.
37. Yoshida M, Cran DG, Pursel VG. Confocal and fluorescence microscopic study using lectins of the distribution of cortical granules during the maturation and fertilization of pig oocytes. *Mol Reprod Dev.* 1993;36:462–8.
38. Mortimer D, Curtis EF, Miller RG. Specific labelling by peanut agglutinin of the outer acrosomal membrane of the human spermatozoon. *J Reprod Fertil.* 1987;81:127–35.
39. Ruggeri E, DeLuca KF, Galli C, Lazzari G, DeLuca JG, Stokes JE, et al. Use of confocal microscopy to evaluate equine zygote development after sperm injection of oocytes matured in vivo or in vitro. *Microsc Microanal.* 2017;23:1197–206.
40. Faramarzi A, Khalili MA, Micara G, Agha-Rahimi A. Revealing the secret life of pre-implantation embryos by time-lapse monitoring: a review. *Int J Reprod Biomed (Yazd).* 2017;15:257–64.
41. Gomez-Torres MJ, Ten J, Girela JL, Romero J, Bernabeu R, De Juan J. Sperm immobilized before intracytoplasmic sperm injection undergo ultrastructural damage and acrosomal disruption. *Fertil Steril.* 2007;88:702–4.
42. Takeuchi T, Colombero LT, Neri QV, Rosenwaks Z, Palermo GD. Does ICSI require acrosomal disruption? An ultrastructural study. *Hum Reprod.* 2004;19:114–7.
43. Ramalho-Santos J, Sutovsky P, Simerly C, Oko R, Wessel GM, Hewitson L, et al. ICSI choreography: fate of sperm structures after monospermic rhesus ICSI and first cell cycle implications. *Hum Reprod.* 2000;15:2610–20.
44. Katayama M, Koshida M, Miyake M. Fate of the acrosome in ooplasm in pigs after IVF and ICSI. *Hum Reprod.* 2002;17:2657–64.
45. Sathananthan AH, Szell A, Ng SC, Kausche A, Lacham-Kaplan O, Trounson A. Is the acrosome reaction a prerequisite for sperm incorporation after intra-cytoplasmic sperm injection (ICSI)? *Reprod Fertil Dev.* 1997;9:703–9.
46. Bourgain C, Nagy ZP, De Zutter H, Van Ranst H, Nogueira D, Van Steirteghem AC. Ultrastructure of gametes after intracytoplasmic sperm injection. *Hum Reprod.* 1998;13(Suppl 1):107–16.
47. Sutovsky P, Hewitson L, Simerly CR, Tengowski MW, Navara CS, Haavisto A, et al. Intracytoplasmic sperm injection for rhesus monkey fertilization results in unusual chromatin, cytoskeletal, and membrane events, but eventually leads to pronuclear development and sperm aster assembly. *Hum Reprod.* 1996;11:1703–12.
48. Enders AC, Liu IK, Bowers J, Lantz KC, Schlafke S, Suarez S. The ovulated ovum of the horse: cytology of nonfertilized ova to pronuclear stage ova. *Biol Reprod.* 1987;37:453–66.

49. Abbott AL, Ducibella T. Calcium and the control of mammalian cortical granule exocytosis. *Front Biosci.* 2001;6:D792–806.
50. Liu M. The biology and dynamics of mammalian cortical granules. *Reprod Biol Endocrinol : RB & E.* 2011;9:149.
51. Bello OD, Cappa AI, de Paola M, Zanetti MN, Fukuda M, Fissore RA, et al. Rab3A, a possible marker of cortical granules, participates in cortical granule exocytosis in mouse eggs. *Exp Cell Res.* 2016;347:42–51.
52. Sun FZ, Bradshaw JP, Galli C, Moor RM. Changes in intracellular calcium concentration in bovine oocytes following penetration by spermatozoa. *J Reprod Fertil.* 1994;101:713–9.
53. Fujimoto S, Yoshida N, Fukui T, Amanai M, Isobe T, Itagaki C, et al. Mammalian phospholipase C ζ induces oocyte activation from the sperm perinuclear matrix. *Dev Biol.* 2004;274:370–83.
54. Bedford-Guaus SJ, McPartlin LA, Xie J, Westmiller SL, Buffone MG, Roberson MS. Molecular cloning and characterization of phospholipase C zeta in equine sperm and testis reveals species-specific differences in expression of catalytically active protein. *Biol Reprod.* 2011;85:78–88.
55. Bedford-Guaus SJ, Yoon SY, Fissore RA, Choi YH, Hinrichs K. Microinjection of mouse phospholipase C zeta complementary RNA into mare oocytes induces long-lasting intracellular calcium oscillations and embryonic development. *Reprod Fertil Dev.* 2008;20:875–83.
56. Betteridge KJ, Eaglesome MD, Mitchell D, Flood PF, Bériault R. Development of horse embryos up to twenty two days after ovulation: observations on fresh specimens. *J Anat.* 1982;135:191–209.
57. Hinrichs K, Love CC, Brinsko SP, Choi YH, Varner DD. In vitro fertilization of in vitro-matured equine oocytes: effect of maturation medium, duration of maturation, and sperm calcium ionophore treatment, and comparison with rates of fertilization in vivo after oviductal transfer. *Biol Reprod.* 2002;67:256–62.
58. Bézard J, Magistrini M, Duchamp G, Palmer E. Chronology of equine fertilisation and embryonic development in vivo and in vitro. *Equine Vet J.* 1989;Supp 8:105–10.
59. Palmer E, Bézard J, Magistrini M, Duchamp G. In vitro fertilisation in the horse: a retrospective study. *J Reprod Fertil.* 1991;44(Supp): 375–84.